

Article

Performance Analysis of Hybrid Radio Frequency and Free Space Optical Communication Networks with Cooperative Spectrum Sharing

Dong Qin ^{1,*}, Yuhao Wang ¹ and Tianqing Zhou ²

¹ School of Information Engineering, Nanchang University, Nanchang 330031, China; wangyuhao@ncu.edu.cn

² School of Information Engineering, East China Jiaotong University, Nanchang 330013, China;

tqzhou@ecjtu.edu.cn

* Correspondence: qindong@seu.edu.cn

Abstract: This paper investigates the impact of cooperative spectrum sharing policy on the performance of hybrid radio frequency and free space optical wireless communication networks, where primary users and secondary users develop a band of the same spectrum resource. The radio frequency links obey Nakagami- m distribution with arbitrary fading parameter m , while the free space optical link follows gamma-gamma distributed atmospheric turbulence with nonzero pointing error. Because the secondary users access the spectrum band without payment, their behavior needs to be restricted. Specifically, the power of the secondary users is dominated by the tolerable threshold of the primary users. Considering both heterodyne and intensity modulation/direct detection strategies in optical receiver, the performance of optical relaying networks is completely different from that of traditional networks. With the help of bivariable Fox's H function, new expressions for cumulative distribution function of equivalent signal to noise ratio at destination, probability density function, outage probability, ergodic capacity and symbol error probability are built in closed forms.



Citation: Qin, D.; Wang, Y.; Zhou, T. Performance Analysis of Hybrid Radio Frequency and Free Space Optical Communication Networks with Cooperative Spectrum Sharing. *Photonics* **2021**, *8*, 108. <https://doi.org/10.3390/photonics8040108>

Received: 8 February 2021

Accepted: 29 March 2021

Published: 6 April 2021

Publisher's Note: MDPI stays neutral with regard to jurisdictional claims in published maps and institutional affiliations.



Copyright: © 2021 by the authors. Licensee MDPI, Basel, Switzerland. This article is an open access article distributed under the terms and conditions of the Creative Commons Attribution (CC BY) license (<https://creativecommons.org/licenses/by/4.0/>).

Keywords: FSO; decode and forward; gamma-gamma distribution

1. Introduction

The introduction of optical communication technology into a relaying system to form an optical relaying network is one of the current research hotspots. By combining the advantages of both radio frequency (RF) and optical communication technologies, higher rate and lower delay can be achieved by seamless connections. The construction of asymmetrical hybrid RF and optical communication links fills the connection gap between the RF circuit and the optical fiber backbone network. For example, a multihop decode and forward (DF) based free space optical (FSO) network was investigated in [1] employing differentially M-ary phase shift keying constellation over an exponential Weibull distributed atmospheric turbulence channel. According to the transition probability matrix in multihop scenario, the authors of [1] derived an average transition probability in an arbitrary differentially M-ary phase shift keying constellation. The optical communication idea was introduced into an unmanned aerial vehicle based wireless network in [2], where two aerial platforms in a low altitude acted as two relay stations to support air to ground communication links. The optical communication process was assumed to take place between these two relays. In terms of the closed form outage probability, the authors of [2] derived the optimal altitude of the aerial platforms. A Markov chain analysis method was applied in [3] in FSO communications in the context buffer aided serial relays to derive average packet delay, which offered clear insight on the selection of the buffer size and diversity gain. A low density parity check coded method was used in [4] in a DF relaying based FSO network. By Gauss Laguerre quadrature rule, the average bit error rate was achieved in double generalized gamma fading environments. Through professional simulation software OptiSystem 11, the effects of incident background radiation and spontaneous emission noise

on the all optical relaying systems at a data rate of 5 Gb/s were considered in [5] for on off keying and differential phase shift keying constellation. A similar optical link construction was considered in a millimeter wave scenario [6], where a fluctuating two-ray fading model was established in millimeter wave link. A visible light communication (VLC) technology was proposed in a full duplex bidirectional relaying network employing adaptive physical layer network coding [7].

On the other hand, due to the lack of sufficient spectrum resources and high purchase prices, spectrum sharing technology has been proposed as one of the effective ways for the alleviation of the scarcity of spectrum resource. For example, an asymmetric RF and FSO cooperative network with spectrum sharing technology was presented in [8], where a direct RF link was added between source and destination. The authors of [8] provided a partial relay selection strategy and demonstrated the diversity order in the presence of outdated channel state information. Similarly, the imperfect channel information was considered in [9] in a multiple input multiple output RF/FSO cooperative system. A unique aspect in [9] was proportional transmission power at secondary users to ensure the quality of service of primary users. A diversity multiplexing trade off analysis was studied in [10] in FSO spectrum sharing networks, where the trade off was proved independent of the primary users. Orthogonal space time block coded transmission was used in [11] in FSO communications for underlay spectrum sharing scenarios. Dominant receive interference cancellation and adaptive receive interference cancellation were incorporated in [12] in FSO cooperative networks for outage probability analysis, which was used to obtain power allocation approach. Although the above public works study the impact of spectrum sharing policy in optical communication networks, they only focus on the interference imposed on the primary users and neglect the interference imposed on the secondary users. This assumption is obviously not applicable to interference limited networks. The secondary users may be subject to transmission interference from primary and cochannel interferer through RF links.

Inspired by the above observations and considering the shortcomings of the existing literature, this paper pursues a detailed spectrum sharing based hybrid RF and FSO DF relaying networks. The main difference between our paper and previous works is that we consider not only the interference level suffered by the primary user, but also the interference level suffered by the secondary user. In a cognitive radio scenario, most works pay more attention to whether the interference on the primary user is within a reasonable range and whether his quality of service is satisfied, while little attention is paid to the interference suffered by the secondary user. But the primary user is often less restrictive in transmission behavior and owns sufficient transmission power to ensure his quality of service requirements. In this scenario, the influence of interference on the secondary user cannot be simply ignored. Although this problem has been studied in the traditional RF link environment, there is a lack of research specifically aimed at optical communications due to the complex channel model affected by atmospheric turbulence and pointing errors. One exception appears in [12], where only simple Rayleigh channel model is assumed in RF link and only one performance metric outage probability is observed. A comparison of previous works is summarized in Table 1.

The main contribution of this paper lies in the following aspects. (1) A hybrid RF/FSO relaying configuration is constructed for spectrum sharing environment, where the imposed interference on the primary users stipulates the power constraint strategy of the secondary users, while the imposed interference on the secondary users deteriorates the performance, which is often ignored in existing literature; (2) Atmospheric turbulence and pointing errors are incorporated into the optical channel model, which follows a gamma-gamma distribution. Additionally, both heterodyne detection and intensity modulation/direct detection (IM/DD) are considered in a uniformed form; (3) closed form expressions are built for cumulative distribution function, probability density function, outage probability, ergodic capacity and symbol error probability (SEP) in hybrid RF and optical communication channels.

Table 1. A comparison of different works

References	Link Model	Spectrum Sharing	Interference Suffered by Secondary User
[1]	FSO	×	×
[2]	RF / FSO	×	×
[3]	FSO	×	×
[4]	FSO	×	×
[5]	FSO	×	×
[6]	RF / FSO	×	×
[7]	VLC	×	×
[8]	RF / FSO	✓	×
[9]	RF / FSO	✓	×
[10]	RF / FSO	✓	×
[11]	RF / FSO	✓	×
[12]	RF / FSO	✓	✓

The remainder of the paper is organized as follows—the system model is presented in Section 2. Then the exact performance analysis is derived in Section 3. Simulation results under various scenarios and discussion are provided in Section 4, followed by conclusion in Section 5.

2. System Model

Consider a hybrid RF/FSO relaying network in a spectrum sharing environment, where a primary network and a secondary network coexist, as shown in Figure 1. The primary network consists of a pair of transmitter PS and receiver PD , and the secondary network is composed of a secondary source SS , a DF relay station SR , and a secondary destination SD . In order to ensure that the communication quality of the primary network is not affected, the transmission power of the secondary source SS has to be limited to $QN_0/|h_p|^2$, where Q is the tolerable threshold of the primary receiver, h_p is the instantaneous channel coefficient of $SS \rightarrow PD$ link and N_0 is noise variance. Moreover, the relay station SR is assumed to suffer from interference not only from the primary transmitter, but also from I cochannel interfering signals. Neglecting the influence of noise, the instantaneous signal to interference ratio at the relay station SR is given by [8]

$$\gamma_{sr} = \frac{Q|h_s|^2 N_0}{|h_p|^2 \left(\sum_{i=0}^I p_{I,i} |h_{I,i}|^2 \right)}, \quad (1)$$

where h_s means the channel coefficient of $SS \rightarrow SR$ link, $p_{I,i}$ and $h_{I,i}$ denote the transmission power and channel coefficient of the i th cochannel interferer, respectively ($i = 0$ denotes the interference from the primary transmitter). Since the FSO link has the advantage of line of sight communication, the work is concentrating on studying the impact of interference level on the RF link. Because the RF link obeys Nakagami- m fading, the above random variables $|h_s|^2$, $|h_p|^2$ and $|h_{I,i}|^2$ obey the gamma distribution.

On the other hand, the $SR \rightarrow SD$ link is a FSO channel with atmospheric turbulence and pointing error, whose probability density function is given by [13]

$$f_{\gamma_{rd}}(z) = \frac{\xi^2}{r\Gamma(a)\Gamma(b)z} G_{1,3}^{3,0} \left[hab \left(\frac{z}{\mu_r} \right)^{\frac{1}{r}} \middle| \begin{matrix} \xi^2 + 1 \\ \xi^2, a, b \end{matrix} \right] \quad (2)$$

where $G(\cdot)$ is the Meijer's G function ([14], Equation (9.301)) $\Gamma(\cdot)$ is the gamma function (ref. [14], Equation (8.310)) γ_{rd} denotes the instantaneous electrical signal to noise ratio (SNR) received at SD, $h = \xi^2 / (\xi^2 + 1)$, r defines the type of detection techniques, that is, $r = 1$ represents heterodyne detection and $r = 2$ represents IM/DD, the quality ξ is the ratio between the equivalent beam radius at the receiver and the pointing error displacement standard deviation at the receiver. The detailed differences between the two detection techniques are provided in [1,6]. The parameter μ_r denotes the electrical SNR of the FSO link defined as [13]

$$\mu_r = \begin{cases} E(\gamma_{rd}) & r = 1 \\ \frac{E(\gamma_{rd})ab\xi^2(\xi^2+2)}{(a+1)(b+1)(\xi^2+1)^2} & r = 2, \end{cases} \quad (3)$$

where $E(\cdot)$ is expectation operation. The quantities a and b are large scale and small scale scintillation parameters, respectively, which are decided according to the Rytov variance [15]. Then the cumulative distribution function of the instantaneous SNR of $SR \rightarrow SD$ link γ_{rd} is given by [16]

$$\begin{aligned} F_{\gamma_{rd}}(z) &= \frac{\xi^2}{\Gamma(a)\Gamma(b)} G_{2,4}^{3,1} \left[hab \left(\frac{z}{\mu_r} \right)^{\frac{1}{r}} \middle| 1, \xi^2 + 1 \right] \\ &= 1 - \frac{\xi^2}{\Gamma(a)\Gamma(b)} H_{2,4}^{4,0} \left[(hab)^r \frac{z}{\mu_r} \middle| (1, 1), (\xi^2 + 1, r) \right. \\ &\quad \left. (0, 1), (\xi^2, r), (a, r), (b, r), \right] \end{aligned} \quad (4)$$

where $H(\cdot)$ is the Fox's H function ([17], Equation (1.1.1)).

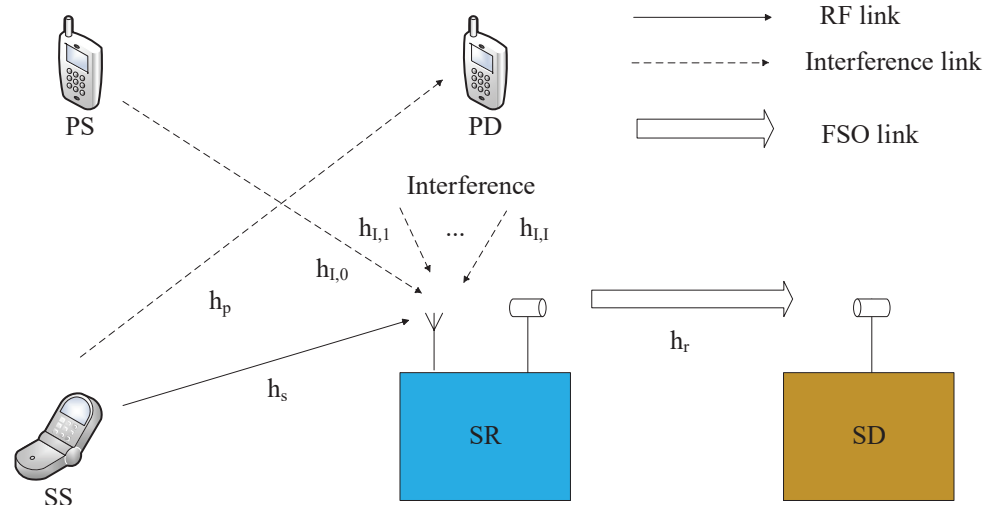


Figure 1. System model.

3. Performance Analysis

In this section, we first discuss the cumulative distribution function and probability density function of the equivalent SNR received by the destination. Then based on the derived cumulative distribution function, we calculate the outage probability, ergodic capacity and SEP of the optical relaying system.

3.1. Outage Probability

According to the DF strategy, the equivalent SNR received by the destination SD is $\gamma = \min(\gamma_{sr}, \gamma_{rd})$. From γ , the cumulative distribution function of γ_{sr} has to be derived first. Denote $V = Q|h_s|^2 / |h_p|^2$, and then cumulative distribution function of V is given by

$$F_v(z) = \int_0^{+\infty} \int_0^{yz} f_{Q|h_s|^2}(x) f_{|h_p|^2}(y) dx dy \\ = 1 - \frac{\beta_{s,2}^{m_{s,2}} \Gamma(m_{s,1} + m_{s,2})}{(\beta_{s,1}z)^{m_{s,2}} \Gamma(m_{s,1}) \Gamma(1 + m_{s,2})} {}_2F_1 \left[\begin{matrix} m_{s,2}, m_{s,1} + m_{s,2}; 1 + m_{s,2} \\ -\frac{\beta_{s,2}}{\beta_{s,1}z} \end{matrix} \right] \quad (5)$$

where $f_x(\cdot)$ is the probability density function of the variable x , $m_{s,1}$ and $m_{s,2}$ are the respective fading parameters of the two variables $Q|h_s|^2$ and $|h_p|^2$, $\beta_{s,1}$ and $\beta_{s,2}$ are the corresponding scale parameters, ${}_2F_1(\cdot)$ is the Gauss hypergeometric function defined in (ref. [14], Equation (9.100)). The probability density function of a typical gamma distribution can be easily found in [8]. Differentiating $F_v(z)$ yields the probability density function of V given by

$$f_v(z) = \frac{\Gamma(m_{s,1} + m_{s,2}) \beta_{s,2}^{m_{s,2}} (\beta_{s,1}z)^{m_{s,1}}}{\Gamma(m_{s,1}) \Gamma(m_{s,2}) z (\beta_{s,1}z + \beta_{s,2})^{m_{s,1} + m_{s,2}}}. \quad (6)$$

For the convenience of analysis, assume that all cochannel interferences experience independent and identically distributed Nakagami- m fading. It is worth noting that if the interferences obey independent and differently distributed Nakagami fading, then the sum of all interferences can still be approximate Nakagami distribution in terms of [18]. Following a similar procedure in V , the cumulative distribution function of γ_{sr} is given by

$$F_{\gamma_{sr}}(z) = 1 - \frac{H_{3,2}^{2,2} \left[\begin{matrix} \beta_{s,1}z \\ \beta_{s,2}\beta_{s,3} \end{matrix} \middle| \begin{matrix} (1 - m_{s,2}, 1), (1 - m_{s,3}, 1), (1, 1) \\ (0, 1), (m_{s,1}, 1) \end{matrix} \right]}{\Gamma(m_{s,1}) \Gamma(m_{s,2}) \Gamma(m_{s,3})} \\ = \frac{H_{3,2}^{1,3} \left[\begin{matrix} \beta_{s,1}z \\ \beta_{s,2}\beta_{s,3} \end{matrix} \middle| \begin{matrix} (1 - m_{s,2}, 1), (1 - m_{s,3}, 1), (1, 1) \\ (m_{s,1}, 1), (0, 1) \end{matrix} \right]}{\Gamma(m_{s,1}) \Gamma(m_{s,2}) \Gamma(m_{s,3})}, \quad (7)$$

where $m_{s,3} = (I + 1)m_I$, m_I denotes the fading parameter of cochannel interference links, and $\beta_{s,3}$ refers to the corresponding scale parameter. Then the probability density function of γ_{sr} is given by

$$f_{\gamma_{sr}}(z) = \frac{H_{2,1}^{1,2} \left[\begin{matrix} \beta_{s,1}z \\ \beta_{s,2}\beta_{s,3} \end{matrix} \middle| \begin{matrix} (1 - m_{s,2}, 1), (1 - m_{s,3}, 1) \\ (m_{s,1}, 1) \end{matrix} \right]}{z \Gamma(m_{s,1}) \Gamma(m_{s,2}) \Gamma(m_{s,3})}. \quad (8)$$

The cumulative distribution function of equivalent SNR $\gamma = \min(\gamma_{sr}, \gamma_{rd})$ is given by

$$F_\gamma(z) = 1 - [1 - F_{sr}(z)][1 - F_{rd}(z)] \\ = 1 - \frac{\xi^2 H_{3,2}^{2,2} \left[\begin{matrix} \beta_{s,1}z \\ \beta_{s,2}\beta_{s,3} \end{matrix} \middle| \begin{matrix} (1 - m_{s,2}, 1), (1 - m_{s,3}, 1), (1, 1) \\ (0, 1), (m_{s,1}, 1) \end{matrix} \right]}{\Gamma(m_{s,1}) \Gamma(m_{s,2}) \Gamma(m_{s,3}) \Gamma(a) \Gamma(b)} \\ \times H_{2,4}^{4,0} \left[\begin{matrix} (hab)^r \frac{z}{\mu_r} \\ \mu_r \end{matrix} \middle| \begin{matrix} (1, 1), (\xi^2 + 1, r) \\ (0, 1), (\xi^2, r), (a, r), (b, r) \end{matrix} \right] \quad (9)$$

The probability density function of γ is written by

$$f_\gamma(z) = \frac{\xi^2 H_{2,1}^{1,2} \left[\begin{array}{c|cc} \beta_{s,1}z & (1-m_{s,2},1), (1-m_{s,3},1) \\ \hline m_{s,1},1 & \end{array} \right] H_{2,4}^{4,0} \left[\begin{array}{c|cc} (hab)^r \frac{z}{\mu_r} & (1,1), (\xi^2+1,r) \\ \hline (0,1), (\xi^2,r), (a,r), (b,r) & \end{array} \right]}{z \Gamma(m_{s,1}) \Gamma(m_{s,2}) \Gamma(m_{s,3}) \Gamma(a) \Gamma(b)} \\ + \frac{\xi^2 G_{1,3}^{3,0} \left[\begin{array}{c|cc} hab \left(\frac{z}{\mu_r} \right)^{\frac{1}{r}} & \xi^2+1 \\ \hline \xi^2, a, b & \end{array} \right] H_{3,2}^{2,2} \left[\begin{array}{c|cc} \beta_{s,1}z & (1-m_{s,2},1), (1-m_{s,3},1), (1,1) \\ \hline (0,1), (m_{s,1},1) & \end{array} \right]}{r \Gamma(m_{s,1}) \Gamma(m_{s,2}) \Gamma(m_{s,3}) \Gamma(a) \Gamma(b) z}. \quad (10)$$

Finally, the outage probability is defined as the probability that the SNR falls below a preset threshold [8]. Using the cumulative distribution function of equivalent SNR γ evaluated at a predefined threshold, the outage probability is written by

$$P_{out} = \Pr(\gamma \leq \gamma_{th}) = F_\gamma(\gamma_{th}), \quad (11)$$

where γ_{th} is a predefined threshold.

3.2. Moments of SNR

The high-order moment of SNR is used to evaluate the level of SNR received by the destination. By using ([17], Equation (2.8.4)), the n th order moment is given by

$$E(\gamma^n) = \int_0^{+\infty} n[1 - F_\gamma(z)]z^{n-1} dz \\ = \frac{n\xi^2\mu_r^n}{\Gamma(m_{s,1})\Gamma(m_{s,2})\Gamma(m_{s,3})\Gamma(a)\Gamma(b)(hab)^{nr}} \\ \times H_{7,4}^{2,6} \left[\begin{array}{c} \beta_{s,1}\mu_r \\ \hline \beta_{s,2}\beta_{s,3}(hab)^r \\ (1-m_{s,2},1), (1-m_{s,3},1), (1-n,1), (1-\xi^2-nr,r), (1-a-nr,r), (1-b-nr,r), (1,1) \\ (0,1), (m_{s,1},1), (-n,1), (-\xi^2-nr,r). \end{array} \right] \quad (12)$$

3.3. Ergodic Capacity

The ergodic capacity is defined as the maximum allowable transmission rate supported by a communication link under which errors are recoverable and is one of the important metrics to measure the communication transmission rate [6]. The ergodic capacity is given by

$$E \left[\frac{1}{2} \log_2(1 + c\gamma) \right] = \frac{c}{2 \ln 2} \int_0^{+\infty} \frac{1 - F_\gamma(x)}{1 + cx} dx, \quad (13)$$

where $c = 1$ for heterodyne detection and $c = e/(2\pi)$ for IM/DD. Unfortunately, the traditional integration method cannot get the result of Equation (13) due to the product of two Meijer's G functions in the cumulative distribution function of γ . We prepare to try the currently prevailing Fox's H function to derive Equation (13). In terms of ([17], Equation (2.9.5)), $1/(1+cx)$ is rewritten as

$$\frac{1}{1+cx} = H_{1,1}^{1,1} \left[cx \middle| \begin{array}{c} (0,1) \\ (0,1). \end{array} \right] \quad (14)$$

By using the integral table ([19], Equation (2.5.1)), the closed formula of ergodic capacity is given by

$$E \left[\frac{\log_2(1 + c\gamma)}{2} \right] = \frac{c\xi^2\mu_r H}{2 \ln 2 \Gamma(m_{s,1})\Gamma(m_{s,2})\Gamma(m_{s,3})\Gamma(a)\Gamma(b)(hab)^r}, \quad (15)$$

where

$$H = H_{4,(3:1),2,(2:1)}^{4,2,1,2,1} \left[\begin{array}{c|c} \frac{\beta_{s,1}\mu_r}{\beta_{s,2}\beta_{s,3}(hab)^r} & \begin{array}{l} (1,1), (\xi^2 + r, r), (a+r, r), (b+r, r) \\ (1-m_{s,2}, 1), (1-m_{s,3}, 1), (1, 1); (0, 1) \\ (2, 1), (\xi^2 + r + 1, r) \\ (0, 1), (m_{s,1}, 1); (0, 1), \end{array} \\ \hline \frac{\xi^2\mu_r}{(hab)^r} & \end{array} \right] \quad (16)$$

where $H(x, y)$ is the bivariable Fox's H function.

3.4. Average Symbol Error Probability

Regarding the error probability, there are generally two expressions. One involves incomplete gamma function for binary modulation, and the other involves Gaussian function for multi-ary modulation. We first set out to start with the binary modulation constellation [1], whose error probability is given by

$$P_e = \frac{\Gamma(p, q\gamma)}{2\Gamma(p)}, \quad (17)$$

where p and q are modulation parameters. For instance, $p = 0.5, q = 0.5$ are for coherent binary frequency shift keying (BFSK) and $p = 0.5, q = 1$ are for coherent binary phase shift keying (BPSK) modulation schemes and so on. According to the characteristics of the DF protocol, the bit error probability is related to the decoding operation at the relay station and the destination. At the relay station, the average bit error probability of the RF link is given by

$$\bar{P}_{e1} = \frac{q^p}{2\Gamma(p)} \int_0^{+\infty} e^{-qx} x^{p-1} F_{\gamma_{sr}}(x) dx \\ = \frac{1}{2} - \frac{H_{4,2}^{2,3} \left[\begin{array}{c} \frac{\beta_{s,1}}{\beta_{s,2}\beta_{s,3}q} \\ \hline (1-m_{s,2}, 1), (1-m_{s,3}, 1), (1-p, 1), (1, 1) \\ (0, 1), (m_{s,1}, 1) \end{array} \right]}{2\Gamma(p)\Gamma(m_{s,1})\Gamma(m_{s,2})\Gamma(m_{s,3})}. \quad (18)$$

Similarly, by using ([14], Equation (7.811.4)), the average bit error probability of optical communication link is given by

$$\bar{P}_{e2} = \frac{q^p}{2\Gamma(p)} \int_0^{+\infty} e^{-qx} x^{p-1} F_{\gamma_{rd}}(x) dx \\ = \frac{1}{2} - \frac{\xi^2 H_{3,4}^{4,1} \left[\begin{array}{c} \frac{(hab)^r}{\mu_r q} \\ \hline (1-p, 1), (1, 1), (\xi^2 + 1, r) \\ (0, 1), (\xi^2, r), (a, r), (b, r) \end{array} \right]}{2\Gamma(p)\Gamma(a)\Gamma(b)}. \quad (19)$$

Finally, the average bit error probability is given by $\bar{P}_e = \bar{P}_{e1} + \bar{P}_{e2} - 2\bar{P}_{e1}\bar{P}_{e2}$ [20].

Next, we turn to the study of multi-ary modulation. In [21], the average SEP of general order rectangular $M_I \times M_Q$ quadrature amplitude modulation (QAM) is given by

$$P_{e,QAM} = 2 \left(1 - \frac{1}{M_I} \right) Q(\sqrt{q_1\gamma}) + 2 \left(1 - \frac{1}{M_Q} \right) Q(\sqrt{q_2\gamma}) \\ - 4 \left(1 - \frac{1}{M_I} \right) \left(1 - \frac{1}{M_Q} \right) Q(\sqrt{q_1\gamma}) Q(\sqrt{q_2\gamma}), \quad (20)$$

where $Q(\cdot)$ is the Gaussian Q function, M_I and M_Q are the dimensions of the in phase and the quadrature components. The qualities q_1 and q_2 is defined as

$$q_1 = \frac{6}{M_I^2 - 1 + (M_Q^2 - 1)r_{QI}^2} \quad (21)$$

$$q_2 = \frac{6r_{QI}^2}{M_I^2 - 1 + (M_Q^2 - 1)r_{QI}^2}, \quad (22)$$

where r_{QI} is the quadrature to in phase decision distance ratio.

At the relay station, the average SEP of the RF link involving a single Gaussian Q function is given by

$$E_{\gamma_{sr}}[Q(\sqrt{q}\gamma)] = \frac{1}{2} - \frac{H_{4,2}^{2,3} \left[\begin{array}{c|c} \frac{2\beta_{s,1}}{\beta_{s,2}\beta_{s,3}q} & (1-m_{s,2}, 1), (1-m_{s,3}, 1), (\frac{1}{2}, 1)(1, 1) \\ \hline (0, 1), (m_{s,1}, 1) \end{array} \right]}{2\sqrt{\pi}\Gamma(m_{s,1})\Gamma(m_{s,2})\Gamma(m_{s,3})}. \quad (23)$$

Using the identity in ([19], Equation (2.5.1)), the average SEP of the RF link involving the product of two Gaussian Q functions is given by

$$\begin{aligned} E_{\gamma_{sr}}[Q(\sqrt{q_1x})Q(\sqrt{q_2x})] &= \int_0^{+\infty} \frac{\sqrt{q_2}e^{-\frac{q_2x}{2}}erfc(\sqrt{\frac{q_1x}{2}}) + \sqrt{q_1}e^{-\frac{q_1x}{2}}erfc(\sqrt{\frac{q_2x}{2}})}{4\sqrt{2\pi x}} F_{\gamma_{sr}}(x) dx \\ &= \frac{1}{2\pi} \left[\arctan\left(\sqrt{\frac{q_1}{q_2}}\right) + \arctan\left(\sqrt{\frac{q_2}{q_1}}\right) \right] - \frac{1}{4\pi\Gamma(m_{s,1})\Gamma(m_{s,2})\Gamma(m_{s,3})} \\ &\times \left\{ H_{1,(1:3),0,(2:2)}^{1,0,2,2,2} \left[\begin{array}{c|c} \frac{q_1}{2\beta_{s,1}} & (\frac{1}{2}, 1) \\ \hline \frac{q_2}{\beta_{s,2}\beta_{s,3}q_2} & (1, 1); (1-m_{s,2}, 1), (1-m_{s,3}, 1), (1, 1) \\ \hline & - \\ & (\frac{1}{2}, 1), (0, 1); (0, 1), (m_{s,1}, 1) \end{array} \right] \right. \\ &+ H_{1,(1:3),0,(2:2)}^{1,0,2,2,2} \left[\begin{array}{c|c} \frac{q_2}{2\beta_{s,1}} & (\frac{1}{2}, 1) \\ \hline \frac{q_1}{\beta_{s,2}\beta_{s,3}q_1} & (1, 1); (1-m_{s,2}, 1), (1-m_{s,3}, 1), (1, 1) \\ \hline & - \\ & (\frac{1}{2}, 1), (0, 1); (0, 1), (m_{s,1}, 1). \end{array} \right] \left. \right\} \quad (24) \end{aligned}$$

Combining the two results in Equations (23) and (24), the average SEP of RF link is expressed as

$$\begin{aligned} \bar{P}_{el,QAM} &= 2\left(1 - \frac{1}{M_I}\right) \left\{ \frac{1}{2} - \frac{H_{4,2}^{2,3} \left[\begin{array}{c|c} \frac{2\beta_{s,1}}{\beta_{s,2}\beta_{s,3}q_1} & (1-m_{s,2}, 1), (1-m_{s,3}, 1), (\frac{1}{2}, 1)(1, 1) \\ \hline (0, 1), (m_{s,1}, 1) \end{array} \right]}{2\sqrt{\pi}\Gamma(m_{s,1})\Gamma(m_{s,2})\Gamma(m_{s,3})} \right\} \\ &+ 2\left(1 - \frac{1}{M_Q}\right) \left\{ \frac{1}{2} - \frac{H_{4,2}^{2,3} \left[\begin{array}{c|c} \frac{2\beta_{s,1}}{\beta_{s,2}\beta_{s,3}q_2} & (1-m_{s,2}, 1), (1-m_{s,3}, 1), (\frac{1}{2}, 1)(1, 1) \\ \hline (0, 1), (m_{s,1}, 1) \end{array} \right]}{2\sqrt{\pi}\Gamma(m_{s,1})\Gamma(m_{s,2})\Gamma(m_{s,3})} \right\} \\ &- 4\left(1 - \frac{1}{M_I}\right)\left(1 - \frac{1}{M_Q}\right) \left\{ \frac{1}{2\pi} \left[\arctan\left(\sqrt{\frac{q_1}{q_2}}\right) + \arctan\left(\sqrt{\frac{q_2}{q_1}}\right) \right] - \frac{1}{4\pi\Gamma(m_{s,1})\Gamma(m_{s,2})\Gamma(m_{s,3})} \right. \\ &\times \left. H_{1,(1:3),0,(2:2)}^{1,0,2,2,2} \left[\begin{array}{c|c} \frac{q_1}{2\beta_{s,1}} & (\frac{1}{2}, 1) \\ \hline \frac{q_2}{\beta_{s,2}\beta_{s,3}q_2} & (1, 1); (1-m_{s,2}, 1), (1-m_{s,3}, 1), (1, 1) \\ \hline & - \\ & (\frac{1}{2}, 1), (0, 1); (0, 1), (m_{s,1}, 1) \end{array} \right] \right. \\ &+ H_{1,(1:3),0,(2:2)}^{1,0,2,2,2} \left[\begin{array}{c|c} \frac{q_2}{2\beta_{s,1}} & (\frac{1}{2}, 1) \\ \hline \frac{q_1}{\beta_{s,2}\beta_{s,3}q_1} & (1, 1); (1-m_{s,2}, 1), (1-m_{s,3}, 1), (1, 1) \\ \hline & - \\ & (\frac{1}{2}, 1), (0, 1); (0, 1), (m_{s,1}, 1). \end{array} \right] \left. \right\} \quad (25) \end{aligned}$$

Similarly, the average SEP of the optical communication link involving a single Gaussian Q function is given by

$$\begin{aligned} E_{\gamma_{rd}}[Q(\sqrt{q}\bar{x})] &= \int_0^{+\infty} \frac{\sqrt{q}e^{-\frac{q}{2}}}{2\sqrt{2\pi}\bar{x}} F(x)dx \\ &= \frac{1}{2} - \frac{\xi^2 H_{3,4}^{4,1} \left[\frac{2(hab)^r}{\mu_r q} \middle| \begin{array}{l} \left(\frac{1}{2}, 1\right), (1, 1), (\xi^2 + 1, r) \\ (0, 1), (\xi^2, r), (a, r), (b, r) \end{array} \right]}{2\sqrt{\pi}\Gamma(a)\Gamma(b)}. \end{aligned} \quad (26)$$

The average SEP of the optical communication link involving the product of two Gaussian Q functions is given by

$$\begin{aligned} E_{\gamma_{rd}}[Q(\sqrt{q_1}\bar{x})Q(\sqrt{q_2}\bar{x})] &= \int_0^{+\infty} \frac{\sqrt{q_2}e^{-\frac{q_2}{2}}\text{erfc}\left(\sqrt{\frac{q_1}{2}}\right) + \sqrt{q_1}e^{-\frac{q_1}{2}}\text{erfc}\left(\sqrt{\frac{q_2}{2}}\right)}{4\sqrt{2\pi}\bar{x}} F(x)dx \\ &= \frac{1}{2\pi} \left[\arctan\left(\sqrt{\frac{q_1}{q_2}}\right) + \arctan\left(\sqrt{\frac{q_2}{q_1}}\right) \right] - \frac{\xi^2}{4\pi\Gamma(a)\Gamma(b)} \\ &\times \left\{ H_{1,(1:2),0,(2:4)}^{1,0,0,2,4} \left[\begin{array}{c} \frac{q_1}{q_2} \\ \frac{2(hab)^r}{\mu_r q_2} \end{array} \middle| \begin{array}{l} \left(\frac{1}{2}, 1\right) \\ (1, 1); (1, 1), (\xi^2 + 1, r) \\ \vdots \\ \left(\frac{1}{2}, 1\right), (0, 1); (0, 1), (\xi^2, r), (a, r), (b, r) \end{array} \right] \right. \\ &+ H_{1,(1:2),0,(2:4)}^{1,0,0,2,4} \left[\begin{array}{c} \frac{q_2}{q_1} \\ \frac{2(hab)^r}{\mu_r q_1} \end{array} \middle| \begin{array}{l} \left(\frac{1}{2}, 1\right) \\ (1, 1); (1, 1), (\xi^2 + 1, r) \\ \vdots \\ \left(\frac{1}{2}, 1\right), (0, 1); (0, 1), (\xi^2, r), (a, r), (b, r). \end{array} \right] \left. \right\} \end{aligned} \quad (27)$$

Combining the two results in Equations (26) and (27), the average SEP of optical communication link is expressed by

$$\begin{aligned} \bar{P}_{e2,QAM} &= 2\left(1 - \frac{1}{M_I}\right) \left\{ \frac{1}{2} - \frac{\xi^2}{2\sqrt{\pi}\Gamma(a)\Gamma(b)} H_{3,4}^{4,1} \left[\frac{2(hab)^r}{\mu_r q_1} \middle| \begin{array}{l} \left(\frac{1}{2}, 1\right), (1, 1), (\xi^2 + 1, r) \\ (0, 1), (\xi^2, r), (a, r), (b, r) \end{array} \right] \right\} \\ &+ 2\left(1 - \frac{1}{M_Q}\right) \left\{ \frac{1}{2} - \frac{\xi^2}{2\sqrt{\pi}\Gamma(a)\Gamma(b)} H_{3,4}^{4,1} \left[\frac{2(hab)^r}{\mu_r q_2} \middle| \begin{array}{l} \left(\frac{1}{2}, 1\right), (1, 1), (\xi^2 + 1, r) \\ (0, 1), (\xi^2, r), (a, r), (b, r) \end{array} \right] \right\} \\ &- 4\left(1 - \frac{1}{M_I}\right)\left(1 - \frac{1}{M_Q}\right) \left\{ \frac{1}{2\pi} \left[\arctan\left(\sqrt{\frac{q_1}{q_2}}\right) + \arctan\left(\sqrt{\frac{q_2}{q_1}}\right) \right] - \frac{\xi^2}{4\pi\Gamma(a)\Gamma(b)} \right. \\ &\times \left. H_{1,(1:2),0,(2:4)}^{1,0,0,2,4} \left[\begin{array}{c} \frac{q_1}{q_2} \\ \frac{2(hab)^r}{\mu_r q_2} \end{array} \middle| \begin{array}{l} \left(\frac{1}{2}, 1\right) \\ (1, 1); (1, 1), (\xi^2 + 1, r) \\ \vdots \\ \left(\frac{1}{2}, 1\right), (0, 1); (0, 1), (\xi^2, r), (a, r), (b, r) \end{array} \right] \right. \\ &+ H_{1,(1:2),0,(2:4)}^{1,0,0,2,4} \left[\begin{array}{c} \frac{q_2}{q_1} \\ \frac{2(hab)^r}{\mu_r q_1} \end{array} \middle| \begin{array}{l} \left(\frac{1}{2}, 1\right) \\ (1, 1); (1, 1), (\xi^2 + 1, r) \\ \vdots \\ \left(\frac{1}{2}, 1\right), (0, 1); (0, 1), (\xi^2, r), (a, r), (b, r). \end{array} \right] \left. \right\} \end{aligned} \quad (28)$$

Finally, combining the results in Equations (25) and (28), the average SEP is approximately as $\bar{P}_{e,QAM} = \bar{P}_{e1,QAM} + \bar{P}_{e2,QAM} - 2\bar{P}_{e1,QAM}\bar{P}_{e2,QAM}$.

So far we have completed the entire performance analysis process. Although our formulas look a bit complicated, the calculation is simple if the idea is clear. First, the integral region is divided according to the decode and forward protocol, and then the cumulative distribution function and probability density function of the equivalent SNR are calculated

in terms of integral table. According to the obtained cumulative distribution function, the corresponding performance expressions are further obtained. Because all formulas are closed, the results can be obtained directly by substituting the corresponding parameter values. Finally, a flow chart is shown in Figure 2 for the purpose of clarity and search.

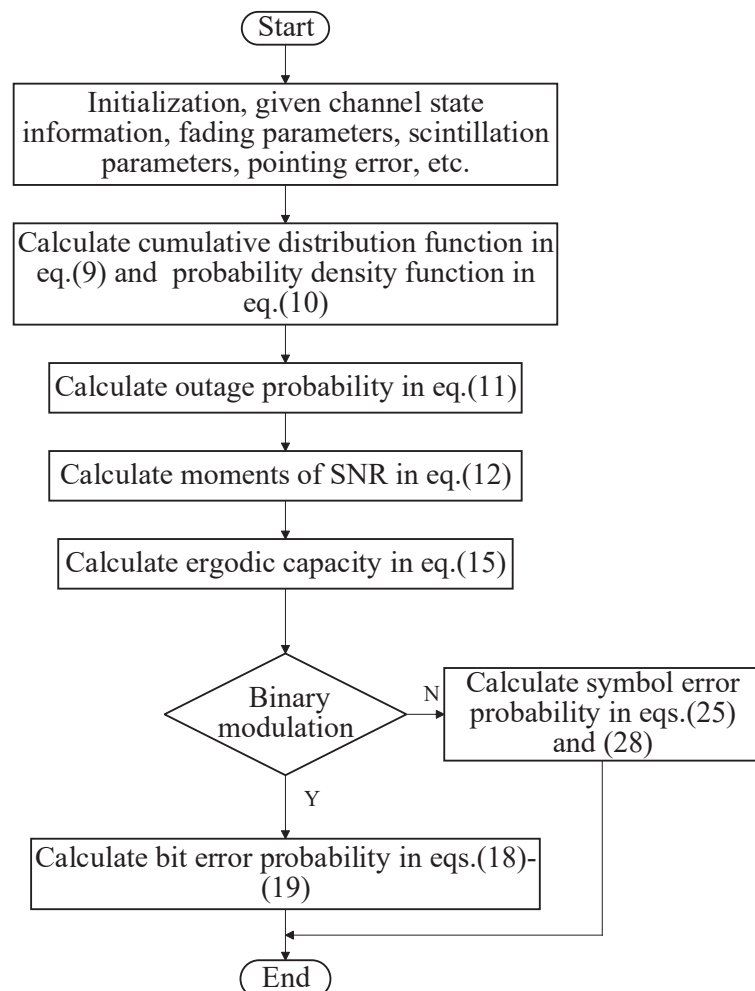


Figure 2. The flow chart of performance analysis procedure.

4. Simulation Results and Discussion

The obtained results above are used to verify the influence on the performance of the hybrid RF/FSO in distinct atmosphere turbulence conditions and fading parameters. Assume that the fading parameters of the RF channels h_s , h_p and $h_{I,i}$ are $m_{s,1} = 2.2$, $m_{s,2} = 1.1$ and $m_I = 0.5$, respectively. The number of cochannel interferences is set to $I = 2$ and all channel gains are normalized to unit one. The prevail simulation software Matlab is used to generate simulation results, which are averaged over 6,250,000 independent samples. The design of the simulation experiments refers to the high quality references [8–13], which provide a general method for FSO communication simulation.

The influence of various atmospheric turbulence and pointing error conditions on the probability of outage is shown in Figure 3. The turbulence and pointing error parameters are taken from [16,22] for different atmospheric conditions. As expected, the simulation curves perfectly coincide with the theoretical values, which proves the correctness of the outage probability formula in terms of the Fox's H function in Equation (10). It can be seen from Figure 3 that the strong atmosphere turbulence (smaller values of a and b) condition increases the outage probability. The reason is that the SNR received by the optical receiver is relatively small due to the severe atmosphere turbulence.

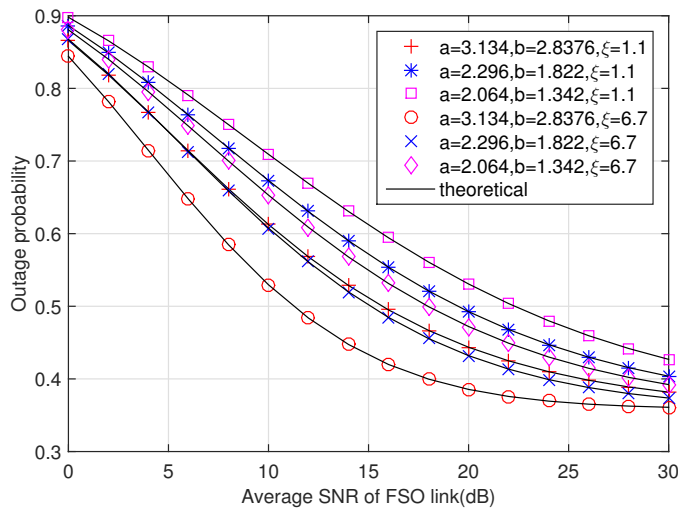


Figure 3. Outage probability under different turbulence and pointing error conditions with IM/DD detection.

Next, the impact of the tolerable interference level of the primary network on the outage probability is illustrated in Figure 4. Unlike the traditional cooperative strategy without spectrum sharing, the outage probability in the cognitive environment does not always decrease with the increasing SNR value. Due to the limitation of interference level of the primary network, the transmission power cannot be increased continuously at the source. So the outage probability always depends on the SNR quality of the worse link.

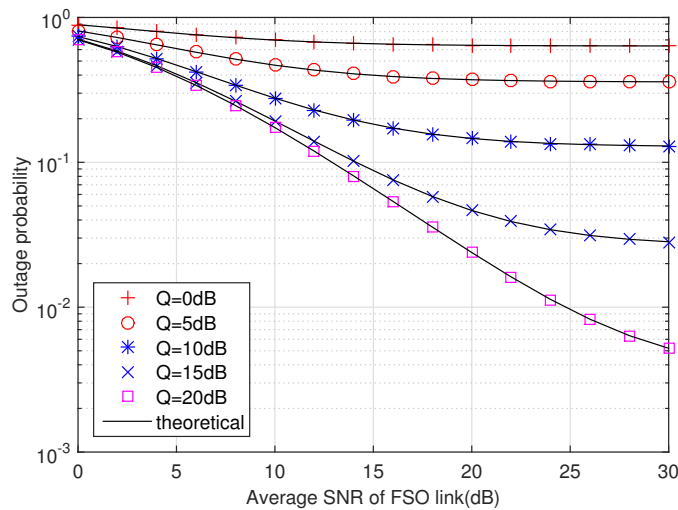


Figure 4. Outage probability under different interference threshold levels with heterodyne detection.

The first order moment of equivalent SNR is plotted in Figure 5. As the tolerable interference level increases, the first order moment also rises. Furthermore, according to Equation (12), the second moment can be drawn similarly. Then the well known amount of fading can be easily obtained as $E(\gamma^2)/E^2(\gamma) - 1$.

Figure 6 shows the ergodic capacity versus average SNR of FSO link, where the interference level is $Q = 5\text{dB}$. It is easy to observe that good channel quality contributes to the increase in ergodic capacity. But when the SNR exceeds a certain level, the growth rate of ergodic capacity slows down. The reason is that when the SNR of the optical link is relative low, the FSO link dominates the capacity and the source has relatively sufficient transmission power. Conversely, when the SNR of the optical link is high, the RF link limits the capacity improvement.

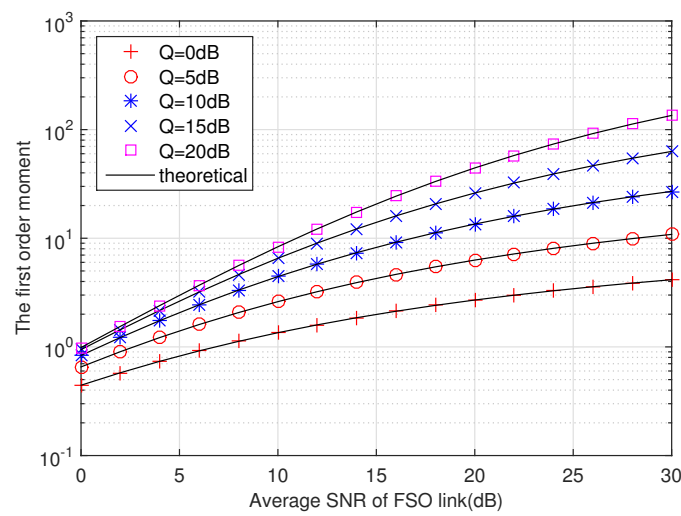


Figure 5. The first order moment of SNR under different interference threshold levels with heterodyne detection.

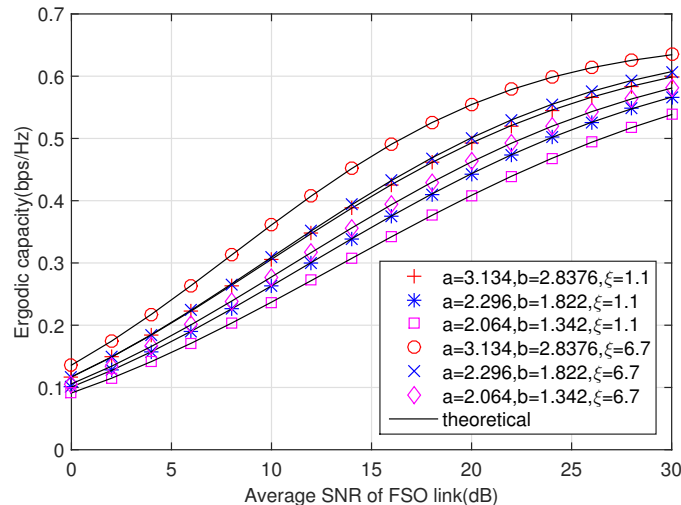


Figure 6. Ergodic capacity under different turbulence and pointing error conditions with IM/DD detection.

The influence of the primary network on the ergodic capacity is drawn in Figure 7. It is clear from Figure 7 that when the SNR of the FSO link exceeds a certain value, the ergodic capacity reaches a saturated state. For example, when the primary network can accept the interference level of no more than 0 dB, the ergodic capacity plateaus at about 20 dB of the FSO link. As the interference level increases, the SNR of the saturation state also raises, indicating the limiting effect of the primary network on the secondary network.

The theoretical error probability formula of coherent BPSK modulation format is shown in Figure 8. Other modulation constellations can be simulated similarly. The relatively small pointing error (large value of ξ) improves the error probability performance. But in the high SNR region, the average error probability curve is not a straight downward line like in traditional cooperative networks. Therefore, the average error probability decreases very slowly, even in the area of high SNR ratio.

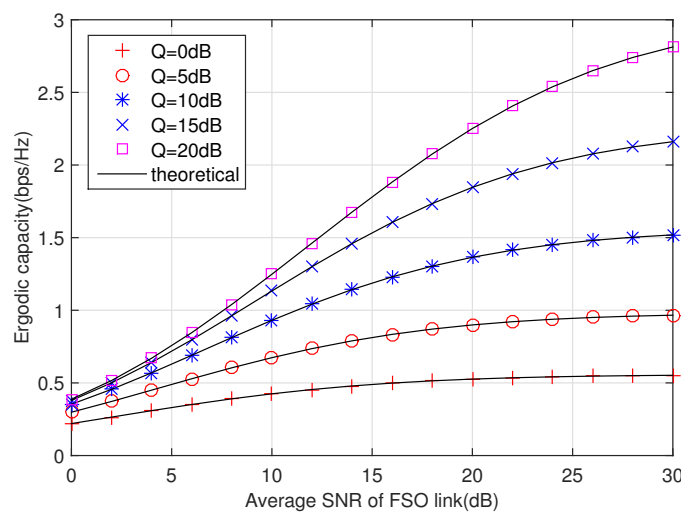


Figure 7. Ergodic capacity under different interference threshold levels with heterodyne detection, where $a = 2.064$, $b = 1.342$ and $\xi = 1.1$.

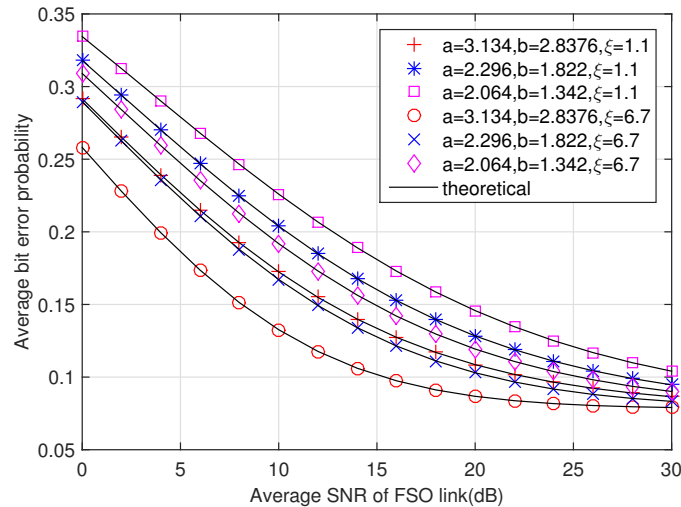


Figure 8. Average bit error probability under different turbulence and pointing error conditions with IM/DD detection, where $Q = 5\text{dB}$.

Finally, the influence of interference level on average bit error probability is plotted in Figure 9. An error floor can be clearly seen from each curve, indicating that the average error probability cannot always be reduced all the time. This is the cost of secondary network accessing unpaid spectrum.

Discussion: At present, the scarcity problem of RF spectrum is becoming increasingly serious due to the growing number of users, wireless access equipment and applications. This has directly led to the widespread application of spectrum sharing technology, making it possible for the majority of secondary users to access the authorized spectrum, as long as the interference generated is within a reasonable range that the primary user can withstand. But the traditional RF link performance has been close to its limit. In this context, the birth of FSO communication has become one of the potential means to enhance wireless capacity due to its high rate characteristic. More importantly, in the cognitive radio environment, FSO communication is more attractive than the RF link because it does not introduce any additional interference to the primary user on the RF link. Therefore, FSO technology is an ideal choice to avoid interference and allow simultaneous communication at primary and secondary users without influence on each other. Based on the above mentioned advantages of FSO communication in spectrum sharing environment, this paper considers a hybrid RF and FSO cooperative communication networks. We are committed

to obtaining precise formulas for common performance to help us accurately grasp the behavior of hybrid cooperative communication networks and avoid a large number of complex repeated experiments.

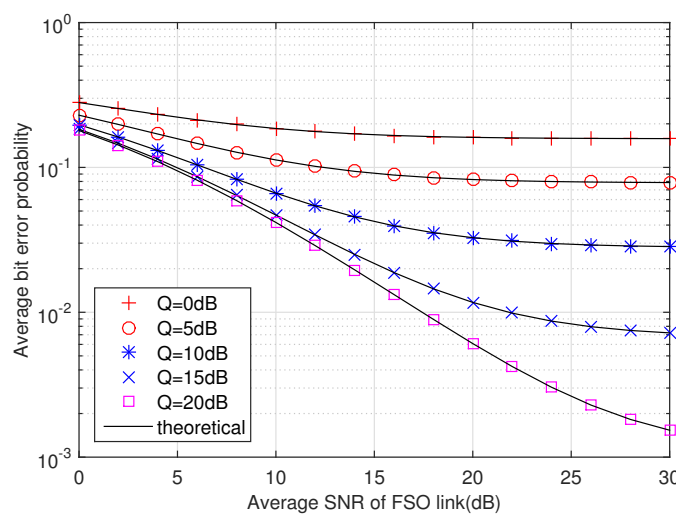


Figure 9. Average bit error probability under different interference threshold levels with heterodyne detection, where $a = 2.064$, $b = 1.342$ and $\xi = 1.1$.

On the other hand, although the spectrum sharing technology has been studied in the traditional RF environment, there is still less discussion in FSO communications. Some references on hybrid RF and FSO cognitive radio cooperative networks tend to ignore the interference received by secondary users [8–11]. The advantage of this assumption is obvious: the SNR received by the secondary user has a simpler form, which lays the foundation for subsequent performance analysis. But we consider a more general scenario and derive more representative and extensive performance formulas. If the interference experienced by the secondary user is not considered as before, the interference amount is just set to zero.

5. Conclusions

This paper has investigated the performance of cooperative hybrid RF/FSO relaying network with spectrum sharing policy in detail. The novel closed-form expressions for cumulative distribution function, probability density function, outage probability, moments of equivalent SNR, ergodic capacity and average SEP are built in terms of Fox's H function. Simulation results demonstrate our theoretical analysis and show the impact of different atmospheric turbulence and pointing error conditions on system performance. Due to the existence of the interference threshold, the relevant performance of the secondary network always reaches a saturated state at high SNR region of FSO link.

Author Contributions: Conceptualization, D.Q.; Methodology, Y.W. and T.Z.; Software, D.Q.; Writing-original draft preparation, D.Q.; Writing-review and editing, Dong Qin. All authors have read and agreed to the published version of the manuscript.

Funding: This work was supported by the National Natural Science Foundation of China under Grant 61761030, Grant No. 62001201 and Grant No. 61861017.

Data Availability Statement: The data used to support the findings of this study are included within the paper.

Conflicts of Interest: The authors declare no conflict of interest.

References

- Agarwal, D.; Bansal, A. Unified error performance of a multihop DF-FSO network with aperture averaging. *J. Opt. Commun. Netw.* **2019**, *11*, 95–106. [[CrossRef](#)]
- Yang, L.; Yuan, J.; Liu, X.; Hasna, M.O. On the performance of LAP-based multiple-hop RF/FSO systems. *IEEE Trans. Aerosp. Electron. Syst.* **2019**, *55*, 499–505. [[CrossRef](#)]
- Abou-Rjeily, C.; Fawaz, W. Buffer-aided serial relaying for FSO communications: Asymptotic analysis and impact of relay placement. *IEEE Trans. Wireless Commun.* **2018**, *17*, 8299–8313. [[CrossRef](#)]
- Jia, C.; Wang, P.; Li, Y.; Huang, C.; Fu, H.; Pang, W. ABERs of LDPC-coded multi-hop FSO over double GG fading channels with pointing error and path loss. *IEEE Photon. Technol. Lett.* **2018**, *30*, 1357–1360. [[CrossRef](#)]
- Huang, X.; Xie, X.; Song, J.; Duan, T.; Hu, H.; Xu, X.; Su, Y. Performance comparison of all-optical amplify-and-forward relaying FSO communication systems with OOK and DPSK modulations. *IEEE Photon. J.* **2018**, *10*, 1–11. [[CrossRef](#)]
- Zhang, Y.; Zhang, J.; Yang, L.; Ai, B.; Alouini, M.-S. On the performance of dual-hop systems over mixed FSO/mmwave fading channels. *IEEE Open J. Commun.* **2020**, *1*, 477–489. [[CrossRef](#)]
- Hong, Y.; Chen, Li.; Zhao, J. Channel-aware adaptive physical-layer network coding over relay-assisted OFDM-VLC networks. *J. Lightw. Technol.* **2020**, *38*, 1168–1177. [[CrossRef](#)]
- Arezumand, H.; Zamiri-jafarian, H.; Soleimani-nasab, E. Exact and asymptotic analysis of partial relay selection for cognitive RF-FSO systems with non-zero boresight pointing errors. *IEEE Access* **2019**, *7*, 58611–59625. [[CrossRef](#)]
- Varshney, N.; Jagannatham, A.K.; Varshney, P. Cognitive MIMO-RF/FSO cooperative relay communication with mobile nodes and imperfect channel state information. *IEEE Trans. Cogn. Commun. Netw.* **2018**, *4*, 544–555. [[CrossRef](#)]
- Arezumand, H.; Zamiri-Jafarian, H.; Soleimani-Nasab, E. Outage and diversity analysis of underlay cognitive mixed RF-FSO cooperative systems. *J. Opt. Commun. Netw.* **2017**, *9*, 909–920. [[CrossRef](#)]
- Varshney, N.; Jagannatham, A.K. Cognitive decode and forward MIMO-RF/FSO cooperative relay networks. *IEEE Commun. Lett.* **2017**, *21*, 893–896. [[CrossRef](#)]
- Al-Qahtani, F.S.; El-Malek, A.H.A.; Ansari, I.; Radaydeh, R.M.; Zummo, S.A. Outage analysis of mixed underlay cognitive RF MIMO and FSO relaying with interference reduction. *IEEE Photon. J.* **2017**, *9*, 1–23. [[CrossRef](#)]
- Zedini, E.; Alouini, M. On the performance of multihop heterodyne FSO systems with pointing errors. *IEEE Photon. J.* **2015**, *7*, 1–10. [[CrossRef](#)]
- Gradshteyn, I.S.; Ryzhik, I.M. *Table of Integrals, Series and Products*, 7th ed.; Academic Press: Cambridge, MA, USA, 2007.
- El-Malek, A.H.A.; Salhab, A.M.; Alouini, S.A.Z.M. Effect of RF interference on the security-reliability tradeoff analysis of multiuser mixed RF/FSO relay networks with power allocation. *J. Lightw. Technol.* **2017**, *35*, 1490–1505. [[CrossRef](#)]
- Ashrafzadeh, B.; Soleimani-Nasab, E.; Uysal, M.K.M. A framework on the performance analysis of dual-hop mixed FSO-RF cooperative systems. *IEEE Trans. Commun.* **2019**, *67*, 4939–4954. [[CrossRef](#)]
- Kilbas, A.A.; Saigo, M. *H-Transforms: Theory and Applications*; CRC Press: Boca Raton, FL, USA, 2004.
- da Costa, D.B.; Ding, H.; Jianhua G. Interference-limited relaying transmissions in dual-hop cooperative networks over Nakagami-m fading. *IEEE Commun. Lett.* **2011**, *15*, 503–505. [[CrossRef](#)]
- Mathai, A.M.; Saxena, R.K.; *The H-Function with Applications in Statistics and Other Disciplines*; John Wiley & Sons: Hoboken, NJ, USA, 1978.
- Deng, Y.; Wang, L.; Elkashlan, M.; Jin Kim, K.; Duong, T.Q. Generalized selection combining for cognitive relay networks over Nakagami-*m* fading. *IEEE Trans. Signal Process.* **2015**, *63*, 1993–2006. [[CrossRef](#)]
- Peppas, K.P.; Datsikas, C.K. Average symbol error probability of general-order rectangular quadrature amplitude modulation of optical wireless communication systems over atmospheric turbulence channels. *J. Opt. Commun. Netw.* **2010**, *2*, 102–110. [[CrossRef](#)]
- Pan, X.; Ran, H.; Pan, G.; Xie, Y.; Zhang, A.J. On secrecy analysis of DF based dual hop mixed RF-FSO systems. *IEEE Access* **2019**, *7*, 66725–66730. [[CrossRef](#)]